Journal of Physics: Condensed Matter

PAPER

Parity of polaritons in a molecular aggregate coupled to a single-mode cavity

To cite this article: Jingyu Liu *et al* 2024 *J. Phys.: Condens. Matter* **36** 115704

View the article online for updates and enhancements.

You may also like

- Exciton-polariton trapping and potential landscape engineering
C Schneider, K Winkler, M D Fraser et al.
- Quantum mechanics of excitation transport in photosynthetic complexes: a key issues review
Federico Levi, Stefano Mostarda, Francesco Rao et al.
- Polariton lasers. Hybrid light–matter lasers without inversion
Daniele Bajoni

This content was downloaded from IP address 221.4.34.130 on 13/12/2023 at 01:35

IOP Publishing Journal of Physics: Condensed Matter
J. Phys.: Condens. Matter **36** (2024) 115704 (8pp) https://doi.org/10.1088/1361-648X/ad1292

Parity of polaritons in a molecular aggregate coupled to a single-mode cavity

Jingyu Liu[1], Jiani Liu[1] and Yao Yao[1,2,*]

[1] Department of Physics, South China University of Technology, Guangzhou 510640, People's Republic of China
[2] State Key Laboratory of Luminescent Materials and Devices, South China University of Technology, Guangzhou 510640, People's Republic of China

E-mail: yaoyao2016@scut.edu.cn

Received 6 October 2023, revised 28 November 2023
Accepted for publication 5 December 2023
Published 12 December 2023

Abstract

We investigated the parity of polaritons, particularly the parity of topological polariton states resulting from light fields, in a molecular aggregate with uniform and alternating excitation transfer interaction coupled to a single-mode cavity. We find that all polariton states are with even parity, in terms of parity conservation, and the even-parity edge states of the Su–Schrieffer–Heeger model with alternating excitation transfer interaction induce even-parity topological polariton states. Thus, the odd-parity edge states are almost unaffected. The original odd-parity edge state is then affected with respect to the parity non-conservation case, i.e. the occupation number of the edge states shifts from one edge to another. This result entails the preparation of edge states from the photonic excited states through an adiabatic process.

Keywords: polaritons, parity, topological polaritons, single-mode cavity, edge states

1. Introduction

Frenkel exciton, an electron–hole pair with a large binding energy [1], emerges as a form of neutral quasiparticle capable of diffusing in semiconductors or molecular polymers [2]. Strong coupling between the exciton and cavity photon produces relatively stable polaritons at room temperature [3, 4]. Due to the small effective mass, polaritons serve as a promising candidate for Bose–Einstein condensation [5, 6]. The energy of the polaritons oscillates repeatedly between excitons and photons, a phenomenon known as Rabi oscillation, with frequencies in organic molecules that can reach record values in the range of $0.1--1\mathrm{eV}/\hbar$ [7–10]. Recently, several works have demonstrated that exciton polaritons play a significant role in organic materials, such as chemical reaction rate [11–15] and energy transport properties [16–20], as well as quantum charging and storage [21, 22].

The concept of topological phase stems from the discovery of the integer quantum Hall effect [23, 24]. The boundary of topological materials gives rise to certain excited states that do not survive in the bulk, though the properties of the boundary are still determined by the bulk, which is known as the bulk-boundary correspondence [25–27]. Recently, the concept of topology has been rapidly extended to various fields in the confined light field systems [28]. One of the fastest growing field is the topological photonics [29, 30], which can simulate a variety of crystal structures by employing photonic crystals [25], optical resonator arrays [31, 32] and waveguides [33]. Further, topological photonics provides a readily achieved platform for the topological phases. Another fast growing field is topological polaritons. Since the energy dispersion of polaritons holds the anti-crossing property, topological polaritons can be observed [34, 35] if the exciton-photon coupling with a phase winding in momentum space and a finite energy gap are realized, where the process is similar to that of obtaining the topological insulators. The proposal of the mechanism of topological polaritons has led to a considerable body of meaningful

* Author to whom any correspondence should be addressed.

© 2023 IOP Publishing Ltd

research, such as the experimental realization of topological polaritons [36–38], topological polariton Laser [39–41] and optical switching [42]. More information on the topological polaritons can be found in the review paper [43]. In addition, certain works have also studied the effects of light field on the topological phases [44, 45].

The representative one-dimensional model exhibiting nontrivial topology is the Su–Schrieffer–Heeger (SSH) model stemming from the studies of polyacetylene [46, 47]. Tuning the nearest neighbor interaction of the SSH model can yield a topologically nontrivial phase, where the bulk topological invariant manifests as a quantized Zak phase [48]. The correspondence between the value of Zak phase and the number of edge states is termed the bulk-boundary correspondence [49]. Combining the SSH model with a confined light field extends the concept of polaritons [45, 50]. Downing *et al* [45] explores the interaction between the SSH model and a multi-mode light field, expanding the original two-dimensional momentum space to a three-dimensional momentum space. Though a bulk-boundary mismatch had been found in the system, an approximation of the reduction of the three-dimensional space back to two-dimensional space has been employed in this work. Jiao *et al* [51] has pointed out that the SSH model with the addition of next-nearest neighbor coupling eliminates chiral symmetry, but the parity conservation still has a certain topological protection for bulk. Furthermore, it was concluded that the correspondence between bulk and boundary does not match. The study in [52] investigated two-dimensional topological polariton states. They break the time-reversal symmetry by manipulating the ratio of left-handed and right-handed light, resulting in an unidirectional transmission edge state. Kozin *et al* [53] utilize polariton rings to construct a one-dimensional zigzag array, obtaining edge states resembling those in the SSH model. Rojas-Sánchez *et al* [54] present a theoretical proposal for achieving the SSH model using Frenkel exciton-polaritons in a one-dimensional lattice of stacked nanocavities at room temperature. Previously, people have focused on the sculpt elaborate crystal lattices to achieve topological polariton. Recently, an all optical controlled polariton SSH system has been experimentally developed [55, 56].

We consider the single-mode light field and deal with the system in real space. Although the idea of the topological bulk-boundary correspondence cannot be followed, certain meaningful phenomena are still found. We found that the polariton states exhibit even parity in the case of parity conservation. The edge states of odd parity are nearly unaffected and have stronger robustness. A method for preparing the edge states is demonstrated from a photon excited states in our work. For the parity non-conservation, we have found that the occupation number of the original odd-parity edge state shifts from one edge to another. The rest of the paper is organized as follows. In section 2, the parity of polariton with uniform excitation transfer interaction has been studied. In section 3, the parity of the SSH model coupled to a single-mode cavity has been investigated. Conclusions and discussions are drawn in section 4.

2. Uniform excitation transfer interaction

We first consider a molecular aggregate consisting of N monomers with uniform excitation transfer interaction located in a single cavity mode microcavity, as sketched in figure 1(a). Since we focus only on the eigenstates and eigenvalues of the system, we neglect all the losses and possible anti-Hermitian terms.

The dispersion of the photonic mode of index m can be expressed as

$$\omega_c\left(q_{\parallel}, m\right) = c\sqrt{q_{\parallel}^2 + (m\pi/L)^2},$$

where c is the speed of light in vacuum and L is the cavity width. For mathematical simplicity, we set the electromagnetic wave vector $\mathbf{q}$ to be the sole component perpendicular to the cavity and the component parallel to the cavity is set to zero, $\mathbf{q}_{\parallel} = 0$, which can be obtained through the discrete states in momentum space of the pillar microcavity. The size of aggregates can be significantly smaller than the wavelength of visible light. For example, the LH2 complex has an approximate size of 7 nm, which is much smaller than the wavelength of visible light [57]. Our focus of study revolves around situations where aggregate sizes are considerably smaller than the wavelength of visible light. Hence, the coupling between each monomer of the molecular aggregate and the light can be approximately treated as identical, which is equivalent to the zero-momentum exciton coupled to the light with $\mathbf{q}_{\parallel} = 0$ [58]. In the subsequent contents, the equation (3) is the Hamiltonian in momentum space, which also shows that, under this assumption, only the zero-momentum exciton states are coupled to the photon states. Under Heitler-London approximation [59] and rotating wave approximation [18], the Hamiltonian of the system can be written as ($\hbar = 1$)

$$\begin{aligned} H &= H_{\mathrm{e}} + H_{\mathrm{c}} + H_{\mathrm{e-c}} \\ H_{\mathrm{e}} &= \sum_n \varepsilon a_n^{\dagger} a_n + \sum_{n \neq m} J a_n^{\dagger} a_m \\ H_{\mathrm{c}} &= \omega_c c^{\dagger} c \\ H_{\mathrm{e-c}} &= g \sum_n \left(a_n^{\dagger} c + c^{\dagger} a_n\right), \end{aligned} \tag{1}$$

where the total Hamiltonian H includes the exciton part H_{e}, cavity mode part H_{c}, and the exciton-cavity coupling part $H_{\mathrm{e\text{-}c}}$. $a_n^{\dagger}$ and a_n are the operators that create and annihilate excitations of the nth monomer with energy ε, respectively. J is the uniform excitation transfer interaction between the nearest-neighbor monomers, which can be seen as the dipole-dipole interaction [59]. $c^{\dagger}$ and c are the photon creation and annihilation operators with energy ω_c, respectively. In practical materials, it is crucial to consider the inhomogeneous broadening resulting from disorder and vibrational degrees of freedom in practical materials. Since the total number of excitations $\sum_n a_n^{\dagger} a_n + c^{\dagger} c$ is conserved, we can work in the single-excitation subspace with $\sum_n a_n^{\dagger} a_n + c^{\dagger} c = 1$. We define the

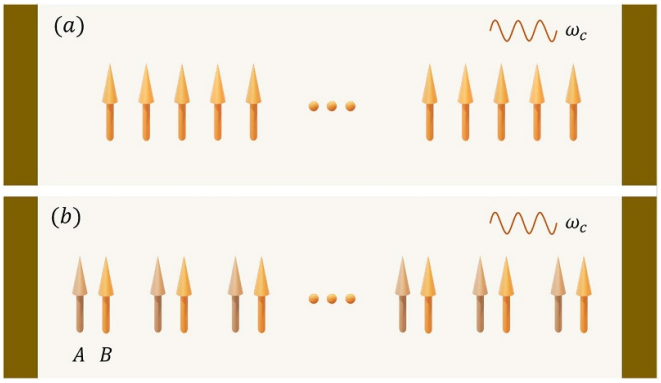

Figure 1. Schematics of molecular aggregates in a single cavity mode microcavity. (a) Uniform excitation transfer interaction between the nearest-neighbor monomers. (b) The dimerized chain with alternating excitation transfer interaction.

basis as $|n\rangle$ and $|c\rangle$ in the single-excitation subspace, where $|n\rangle$ denotes the excited state of the nth monomer and $|c\rangle$ denotes the single-photon state. The difference between the current model and the Tavis-Cummings (TC) [60] or Dicke model [61] lies in the additional excitation transfer interaction. The Hamiltonian can be rewritten as

$$\begin{aligned} H &= H_{\mathrm{e}} + H_{\mathrm{c}} + H_{\mathrm{e-c}} \\ H_{\mathrm{e}} &= \sum_{n=1}^{N} \varepsilon |n\rangle\langle n| + \sum_{n=1}^{N-1} J\left(|n\rangle\langle n+1| + h.c.\right) \\ H_{\mathrm{c}} &= \omega_c |c\rangle\langle c| \\ H_{\mathrm{e-c}} &= g \sum_{n} \left(|n\rangle\langle c| + |c\rangle\langle n|\right). \end{aligned} \tag{2}$$

To better analyze the characteristics of the open-boundary system, we first investigate a cyclic molecular system with its ends connected. In this scenario, we can express the system Hamiltonian in the momentum space using Fourier transforms

$$\begin{aligned} H = &\sum_{k} \left(\varepsilon + 2J\cos k\right) |k\rangle\langle k| + \omega_c |c\rangle\langle c| \\ &+ g\sqrt{N}\left(|k=0\rangle\langle c| + |c\rangle\langle k=0|\right), \end{aligned} \tag{3}$$

where,

$$|k\rangle = \frac{1}{\sqrt{N}} \sum_{n} \mathrm{e}^{ikn} |n\rangle, \ |n\rangle = \frac{1}{\sqrt{N}} \sum_{k} \mathrm{e}^{-ikn} |k\rangle, \tag{4}$$

$k \in \{0,\ \delta_k,\ 2\delta_k,\ \ldots,\ (N-1)\delta_k\}$ with $\delta_k = 2\pi/N$. We observe that solely the bright exciton state, characterized by zero momentum, couples to the cavity photon. By diagonalizing the Hamiltonian, we can obtain

$$H = \sum_{k\neq 0} \left(\varepsilon + 2J\cos k\right) |k\rangle\langle k| + E_{\mathrm{U}} |\mathrm{U}\rangle\langle \mathrm{U}| + E_{\mathrm{L}} |\mathrm{L}\rangle\langle \mathrm{L}|, \tag{5}$$

where,

$$E_{\mathrm{U/L}} = \frac{\varepsilon + 2J + \omega_c \pm \sqrt{\left(\varepsilon + 2J - \omega_c\right)^2 + 4Ng^2}}{2}, \tag{6}$$

$$|\mathrm{U}\rangle = \cos\theta |k=0\rangle + \sin\theta |c\rangle, \ |\mathrm{L}\rangle = \cos\theta |k=0\rangle - \sin\theta |c\rangle,$$

$\tan\theta = \pm\left[\varepsilon + 2J - \omega_c + \sqrt{(\varepsilon + 2J - \omega_c)^2 + 4g^2}\right] / g\sqrt{N}$. The states, $|k \neq 0\rangle$, $|\mathrm{U}\rangle$ and $|\mathrm{L}\rangle$ are known as the dark states, upper polariton state, and lower polariton state, respectively [58, 62]. When $\varepsilon = \omega_c$, and $J = 0$, the polariton states $|\mathrm{U}\rangle = \frac{\sqrt{2}}{2}(|k=0\rangle + |c\rangle)$ and $|\mathrm{L}\rangle = \frac{\sqrt{2}}{2}(|k=0\rangle - |c\rangle)$ are each comprised of half excitons and half photons. Meanwhile, the eigenvalues are reduced to $E_{\mathrm{U/L}} = \varepsilon \pm g\sqrt{N}$, where $g\sqrt{N}$ is a parameter that measures the coupling strength of the whole matter with the light field. $2g\sqrt{N}$ is commonly known as the collective Rabi frequency [17, 58]. Here, $|k=0\rangle$ is a completely symmetric state with respect to the molecular chains so that the polariton states are also even-parity states.

Returning to the finite length chain from the parity point of view, the parity symmetry of the Hamiltonian implies parity conservation. The eigenstates of the parity-conserved system possess either odd parity or even parity. We define a parity operator P, which must satisfy the operation on any state $P\sum_n a_n|n\rangle + a_c|c\rangle = \sum_n a_{N-n+1}|n\rangle + a_c|c\rangle$. Its physical meaning is to symmetrically exchange the position of n with the position of $N-n+1$. Therefore, the expression of the parity operator can be defined as

$$P = \sum_{n=1}^{N} |n\rangle\langle N-n+1| + |c\rangle\langle c|. \tag{7}$$

The parity of the system is conserved for $PHP = H$ or $[P,H] = 0$. Since the single-photon state $|c\rangle$ can be regarded as an even-parity state, the polariton states containing the photon components must also be of even-parity state. Otherwise, the polariton states would be without any parity. For the plane waves basis states of cyclic molecular system, we can derive $P|k\rangle = \mathrm{e}^{ik}|-k\rangle$. The parity operator induces a reversal of momentum direction. To trace these polariton states, we define a mixing ratio for measuring the mixing degree of light and matter for a arbitrary wave function $|\psi\rangle$

$$\eta = \left|\left|2\langle\psi|c\rangle\langle c|\psi\rangle - 1\right| - 1\right|. \tag{8}$$

When $\eta = 1$, an equal distribution between light and matter occurs, resulting in the highest degree of mixing; whereas for $\eta = 0$, there is no mixing between light and matter. Figure 2 shows the energy levels as a function of the exciton-cavity coupling. It is evident that the intersection and anti-intersection always appear alternately. Since the ratio η of the anti-intersection position is large, the two curves of anti-intersection represent the two branches of polaritons. Furthermore, all the polaritons are of even-parity, which is consistent with our prediction.

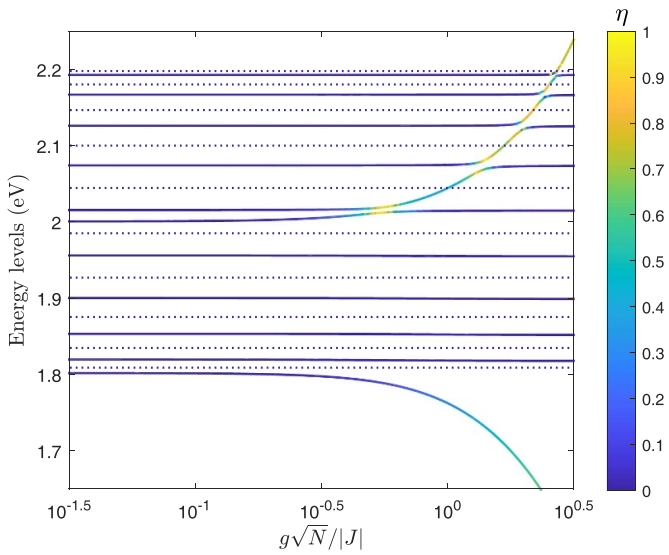

Figure 2. The energy level diagram with a uniform excitation transfer interaction. The solid lines represent the even-parity states whereas the dotted lines represent the odd-parity states. The mixing ratio at the anti-intersection is significantly larger than the intersection. The number of monomers $N = 20$, other parameters $\varepsilon = \omega_c = 2\,\mathrm{eV}$ and $J = -0.1\,\mathrm{eV}$.

3. Non-uniform excitation transfer interaction

In an organic aggregate, the uniform transfer interaction is usually unstable. The process of dimerization can enhance the system's stability, leading to the formation of relatively stable structure known as the SSH model, as sketched in figure 1(b). We define the basis vectors in the single-excitation subspace as $|n,A\rangle$, $|m,B\rangle$, and $|c\rangle$, which represent the excitation state of the A sublattice in dimer n, the B sulattice in dimer m, and the single photon, respectively. The Hamiltonian can be expressed as

$$\begin{aligned} H &= H_{\mathrm{e}} + H_{\mathrm{c}} + H_{\mathrm{e-c}}, \\ H_{\mathrm{e}} &= \sum_{n=1}^{N} \left(\varepsilon_A |n,A\rangle\langle n,A| + \varepsilon_B |n,B\rangle\langle n,B|\right) \\ &\quad + v \sum_{n=1}^{N} \left(|n,B\rangle\langle n,A| + h.c.\right) \\ &\quad + w \sum_{n=1}^{N-1} \left(|n+1,B\rangle\langle n,A| + h.c.\right), \\ H_{\mathrm{c}} &= \omega_c |c\rangle\langle c|, \\ H_{\mathrm{e-c}} &= g_A \sum_{n} \left(|n,A\rangle\langle c| + |c\rangle\langle n,A|\right) \\ &\quad + g_B \sum_{n} \left(|n,B\rangle\langle c| + |c\rangle\langle n,B|\right), \end{aligned} \tag{9}$$

where the dipole interaction within the dimer is v and the dipole interaction between the dimers is w.

3.1. Parity conservation

The parity operator can be defined, similar to that in the previous section, as

$$P_{\mathrm{SSH}} = \sum_{n=1}^{N} \left(|n,A\rangle\langle N-n+1,B| + |n,B\rangle\langle N-n+1,A|\right) + |c\rangle\langle c|. \tag{10}$$

Parity conservation requires that the excitation energy of monomer A is equal to B and that the interaction between the cavity and both monomers are of the same intensity $\mathrm{g_A} = \mathrm{g_B}$. In the pure SSH model, the molecular chain has parity symmetry besides chiral symmetry $\{\Sigma, H-\varepsilon\} = 0$, where the chiral operator can be written as [49]

$$\Sigma = \sum_{n=1}^{N} |n,A\rangle\langle n,A| - |n,B\rangle\langle n,B|. \tag{11}$$

The energy levels of the system with chiral symmetry manifest a symmetric distribution with respect to ε. However, when the SSH model couples to a single mode cavity, the chiral symmetry of the system will be broken $\{\Sigma, H-\varepsilon\} \neq 0$. Therefore, the energy levels will no longer be symmetrically distributed with respect to ε, as shown in figure 3(a).

For the bare SSH model, if $|v| < |w|$, the winding number of the system is 1. In this case, the SSH model is nontrivial, hosting two edge states-one odd-parity state and the other even-parity state. An edge state is a state in which the wave function is localized spatially at the left (right) edge. Given that our considered system incorporates a photon component, the definition of the edge states should exclude the photon component, and therefore can be defined as [49]

$$\sum_{n\in\{1,2,N-1,N\}} \frac{|\langle\psi|n,A\rangle|^2 + |\langle\psi|n,B\rangle|^2}{1-|\langle\psi|c\rangle|^2} > 0.6.$$

Although the photon component is excluded in the formula, we will also find in subsequent calculations that the coupling of light with matter affects the edge states.

When the cavity mode frequency resonates with the edge state energy, the photon will be coupled to the even-parity edge state to form an even-parity edge polariton state, as shown in figures 3(a), (b), and (d). As the exciton-cavity coupling strength increases, the edge state of even parity will slightly deviate from the energy ε. The edge state of odd parity and the other odd-parity states unaffected, as shown in figures 3(a) and (c). This suggests that edge states with odd parity exhibit a stronger resistance to interference within the confined light field system. We declare that the system is a leak-free optical cavity system, which neglects all the losses and possible anti-Hermitian terms. Therefore, as long as a small detuning is given, even though the exciton-cavity coupling is very weak, the mixing of light and matter will be significant. In a leaky optical cavity, however, if the coupling is weak, the lifetime of the photon will be shorter than the period of the conversion

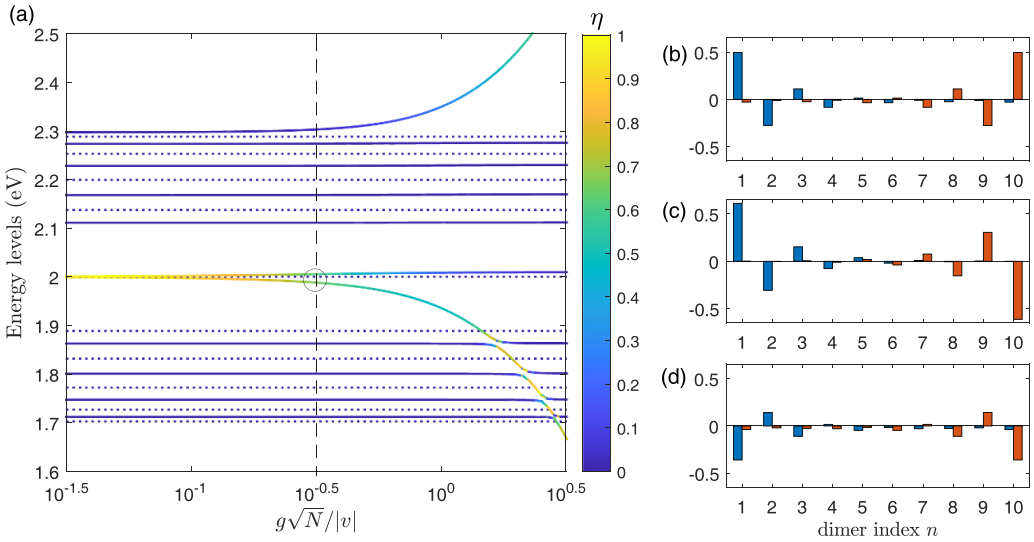

Figure 3. (a) Energy levels of the SSH model coupled to a single-mode cavity with resonant coupling. The solid lines represent even-parity states, whereas the dotted lines represent odd-parity states. The mixing ratio at the anti-intersection is significantly larger than at the intersection. The single photon state only mixes with the even-parity edge states and other even-parity states, forming the polariton states. Panels (b), (c), and (d) display the wave function probability amplitude distribution at three intersection points of the vertical dotted line and the energy level graph, from top to bottom within the small circle. The blue color indicates the A sublattice, while the red color indicates the B sublattice. Panels (b) and (d) depict the two branches of polaritons, both of which are even-parity states. Panel (c) illustrates an odd-parity edge state. The number of dimers $N = 10$, other parameters $\varepsilon = \omega_c = 2\,\text{eV}$, $v = 0.1\,\text{eV}$ and $w = 0.2\,\text{eV}$.

between light and matter, implying that the polariton becomes unstable.

The long-range coupling induced by light is different from that between the dimers, i.e. the long-range coupling between the dimers will lead the edge states to be no longer localized [51]. The light-induced long-range coupling only mixes the photon components into the edge state without changing the edge states. Consequently, the topological polaritons exhibit photon-like characteristics, such as a smaller effective mass and improved transmission properties.

When the cavity mode frequency does not resonate with the edge state energy, the values of photon energy will deviate from that of the edge states energy for the weak exciton-cavity coupling strength, as shown in figure 4. With an increase in exciton-cavity coupling strength, the single-photon state initially transitions to a polariton state and subsequently to the edge state. This transition process can be utilized for edge state preparation: injecting a photon with a frequency surpassing the monomer excitation energy into the cavity, then progressively augmenting the exciton-cavity coupling to enable the single-photon state's adiabatic evolution into an edge state. Notably, the nearly unaffected middle dotted line confirms the robustness of the odd-parity edge state. Meanwhile, the middle solid line delineates the transformation of the even-parity edge state into an even-parity edge polariton state, followed by a transition into a regular even-parity state.

To verify the generation of edge states by the photonic state, we further perform an adiabatic evolution of the system. The initial state of the system is set to the single-photon state $|c\rangle$, and the time-dependent Hamiltonian is set to $H = H(g(t))$, where the exciton-cavity coupling strength increases linearly

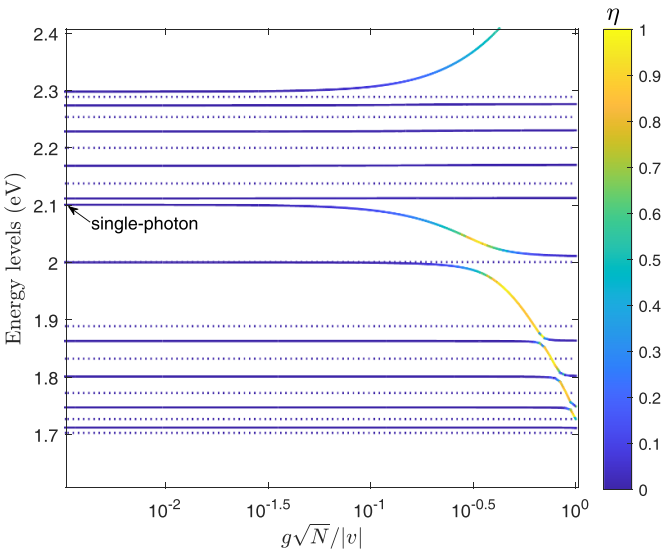

Figure 4. Energy levels of the SSH model coupled to a single mode cavity with non-resonant coupling ($\varepsilon_A = \varepsilon_B \neq \omega_c$). The three middle lines from top to bottom represent the states of single-photon, odd-parity edge, and even-parity edge, respectively. The number of dimers $N = 10$, other parameters $\varepsilon_A = \varepsilon_B = \varepsilon = 2\,\text{eV}$, $\omega_c = 2.1\,\text{eV}$, $v = 0.1\,\text{eV}$ and $w = 0.2\,\text{eV}$.

with time $g(t) = \beta t$, and $\beta = 10^{-4}\,\text{eV}$. According to figure 5, the projection probability of the edge is significantly stronger than that of the other states over time. This suggests that the adiabatic evolution, starting from the single-photon state $|c\rangle$, can evolve to the edge state with a higher probability. We emphasize that the adiabatic evolution, while theoretically

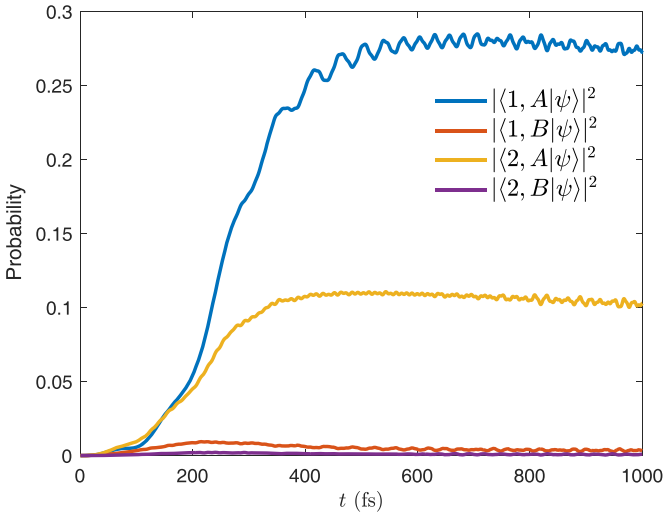

Figure 5. Adiabatic evolution under non-resonant coupling. The exciton-cavity coupling strength increases linearly with time, $g = \beta t$, $\beta = 10^{-4}\,\mathrm{eV\,fs^{-1}}$. The blue, red, yellow, and purple lines represent the projection probability of states $|1,A\rangle$, $|1,B\rangle$, $|2,A\rangle$ and $|2,B\rangle$ respectively. The remaining edge will also take on the shape of the figure symmetrically. Other parameters $N = 10$, $\varepsilon_A = \varepsilon_B = \varepsilon = 2\,\mathrm{eV}$, $\omega_c = 2.05\,\mathrm{eV}$, $v = 0.1\,\mathrm{eV}$ and $w = 0.2\,\mathrm{eV}$.

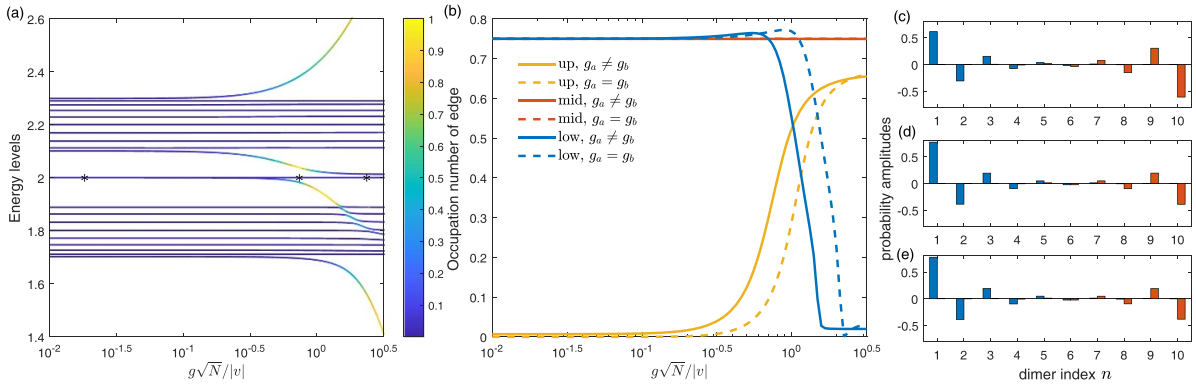

Figure 6. (a) Energy levels with unequal exciton-cavity coupling strength coupled $g_a = 0.5g_b = g$. (b) The yellow, red, and blue solid lines correspond to the three energy levels in the middle of panel (a) respectively. The dashed line is the case where the exciton-cavity field coupling is equal. (c)–(e) Wave function probability amplitude distributions correspond to the asterisk points on the middle line of panel (a) from left to right. Other parameters are same as that in figure 4.

valid, poses significant challenges in practical implementation due to the inhomogeneous broadening resulting from disorder and vibrational degrees of freedom. However, the calculations we have conducted hold significance, and offer at least a preliminary approximation to the experimental observations.

3.2. *Parity non-conservation*

When the excitation energy of monomer A not equal to that of monomer B, i.e. $\varepsilon_A \neq \varepsilon_B$, and the interaction strength of the cavity field with the two monomers is different, i.e. $g_A \neq g_B$, the parity is shown to be not conserved by the parity operator. According to figure 6(a), no energy level crossing appears and all energy levels are anti-crossing, which implies that the parity of the system is no longer conserved. The original odd-parity edge state does not exhibit anti-crossing phenomenon, as indicated by the straight line in the middle of figure 6(a). Figure 6(b) shows that although the occupation number of edge, i.e. [49]

$$\sum_{n=\{1,2,N-1,N\}} \left(|\langle\psi|n,A\rangle|^2 + |\langle\psi|n,B\rangle|^2\right),$$

for this state is nearly unaffected, the occupation number of the edge shifts from one edge to another, as shown in figures 6(c)–(e). Furthermore, the parity non-conservation can also be achieved by changing the structure of molecular aggregates. We then remove the last B monomer and find that only one left edge state exists in this structure in the presence of odd number of monomers, as shown in figure 7. According to figures 7(b) and (d), the introduction of the optical field mixes the left edge states into the extra bulk excitations.

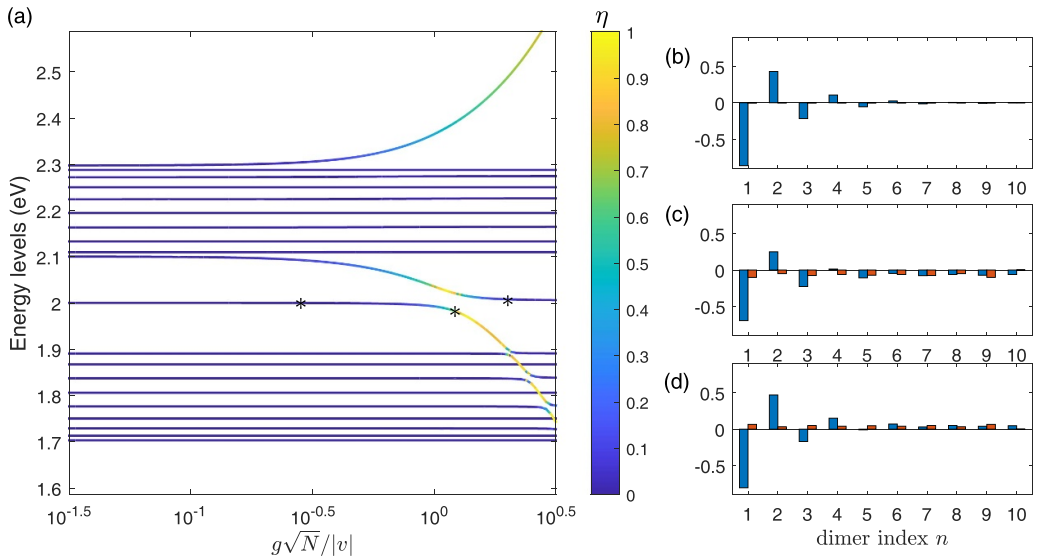

Figure 7. (a) Energy levels for the odd number monomers. (b)–(d) Wave function probability amplitude distributions correspond to the asterisk points on the middle line of panel from left to right. Other parameters are identical to figure 4.

4. Conclusions and discussions

We investigated a molecular aggregate with uniform excitation transfer interaction located in a single cavity mode microcavity. The system possesses parity symmetry, resulting in all polariton states being even-parity states due to the single-photon state's inherent even-parity nature. Furthermore, our exploration involved the SSH model with alternating excitation transfer interaction within a single cavity mode microcavity. Under the constraint of parity conservation, we observed that exciton polariton states exhibit even parity. The coupling of even-parity edge states with photons results in the formation of even-parity polariton states, leaving the odd-parity edge states unaffected. This discovery suggests a novel method for preparing edge states from photonic excited states via an adiabatic process. Under the condition of parity non-conservation, the odd-parity edge states are still edge states though the occupation number of edge shifts from one edge to another. Although the results presented in this work are solely based on the real-space derivation and calculation, our results can guide the designing of organic polariton materials. Introduction of light field provides an additional degree of freedom in comparison to the pure SSH model. It is well known that there are two methods to change the winding number of the SSH model. The first method requires closing the bulk gap, and the second method requires breaking chiral symmetry. By introducing a light field to break the chiral symmetry, it is possible to change the winding number without changing the edge states of the system. This is also a well strategy for breaking the bulk-boundary correspondence. Our research is equivalent to providing a key for matching parity states. By introducing optical fields, we can distinguish between odd and even parity states. This can be directly applied to the detection of quantum states and also has certain application value in the manipulation of topological polaritons with light.

Data availability statement

All data that support the findings of this study are included within the article (and any supplementary files).

Acknowledgments

The authors gratefully acknowledge support from the Key Research and Development Project of Guangdong Province (Grant No. 2020B0303300001), National Natural Science Foundation of China (Grant No. 11974118) and Science and Technology Planning Project of Guangzhou (Grant No. 202201010696).

ORCID iD

Jingyu Liu https://orcid.org/0000-0001-6379-0685

References

[1] Frenkel J 1931 *Phys. Rev.* **37** 1276
[2] May V and Kühn O 2011 *Charge and Energy Transfer Dynamics in Molecular Systems* 3rd edn (Wiley)
[3] Lidzey D G, Bradley D D C, Virgili T, Armitage A, Skolnick M S and Walker S 1999 *Phys. Rev. Lett.* **82** 3316
[4] Lerario1 G *et al* 2017 *Nat. Phys.* **13** 837
[5] Deng H, Haug H and Yamamoto Y 2010 *Rev. Mod. Phys.* **82** 1489
[6] Plumhof J D, Stöferle T, Mai L, Scherf U and Mahrt R F 2014 *Nat. Mater.* **13** 247
[7] Schwartz T, Hutchison J A, Genet C and Ebbesen T W 2011 *Phys. Rev. Lett.* **106** 196405
[8] Kéa-Cohen S, Maier S A and Bradley D D C 2013 *Adv. Opt. Mater.* **1** 827
[9] Mazzeo M *et al* 2014 *Appl. Phys. Lett.* **104** 233303
[10] Ebbesen T W 2016 *Acc. Chem. Res.* **49** 2403

[11] Herrera F and Spano F C 2016 *Phys. Rev. Lett.* **116** 238301
[12] Galego J, Garcia-Vidal F J and Feist J 2016 *Nat. Commun.* **7** 13841
[13] Galego J, Garcia-Vidal F J and Feist J 2017 *Phys. Rev. Lett.* **119** 136001
[14] Garcia-Vidal F J, Ciuti C and Ebbesen T W 2021 *Science* **373** eabd0336
[15] Pannir-Sivajothi S, Campos-Gonzalez-Angulo J A, Martínez-Martínez L A, Sinha S and Yuen-Zhou J 2022 *Nat. Commun.* **13** 1645
[16] Orgiu E *et al* 2015 *Nat. Mater.* **14** 1123
[17] Schachenmayer J, Genes C, Tignone E and Pupillo G 2015 *Phys. Rev. Lett.* **114** 196403
[18] Feist J and Garcia-Vidal F J 2015 *Phys. Rev. Lett.* **114** 196402
[19] Liu J, Zhao Q and Wu N 2019 *J. Chem. Phys.* **150** 105102
[20] Krainova N, Grede A J, Tsokkou D, Banerji N and Giebink N C 2020 *Phys. Rev. Lett.* **124** 177401
[21] Campaioli F, Pollock F A, Binder F C, Céleri L, Goold J, Vinjanampathy S and Modi K 2017 *Phys. Rev. Lett.* **118** 150601
[22] Ferraro D, Campisi M, Andolina G M, Pellegrini V and Polini M 2018 *Phys. Rev. Lett.* **120** 117702
[23] Klitzing K V, Dorda G and Pepper M 1980 *Phys. Rev. Lett.* **45** 494
[24] Klitzing K v 1986 *Rev. Mod. Phys.* **58** 519
[25] Hasan M Z and Kane C L 2010 *Rev. Mod. Phys.* **82** 3045
[26] Qi X L and Zhang S C 2011 *Rev. Mod. Phys.* **83** 1057
[27] Ozawa T, Price H M, Amo A, Goldman N and Carusotto I 2019 *Rev. Mod. Phys.* **91** 015006
[28] Rider M S, Palmer S J, Pocock S R, Xiao X, Arroyo Huidobro P and Giannini V 2019 *J. Appl. Phys.* **125** 120901
[29] Haldane F D M and Raghu S 2008 *Phys. Rev. Lett.* **100** 013904
[30] Raghu S and Haldane F D M 2008 *Phys. Rev.* A **78** 033834
[31] Hafezi M, Mittal S, Fan J and Taylor J M 2013 *Nat. Photon.* **7** 1001
[32] Ningyuan J, Sommer A, Schuster D and Simon J 2015 *Phys. Rev.* X **5** 021031
[33] Rechtsman M C, Zeuner J M, Plotnik Y, Lumer Y, Podolsky D, Dreisow F, Nolte S, Segev M and Szameit A 2013 *Nature* **496** 196
[34] Bardyn C E, Karzig T, Refael G and Liew T C H 2015 *Phys. Rev.* B **91** 161413
[35] Karzig T, Bardyn C E, Lindner N H and Refael G 2015 *Phys. Rev.* X **5** 031001
[36] Klembt S 2018 *Nature* **562** 552
[37] Liu W, Ji Z, Wang Y, Modi G, Hwang M, Zheng B, Sorger V J, Pan A and Agarwal R 2020 *Science* **370** 600
[38] Li M *et al* 2021 *Nat. Commun.* **12** 4425
[39] Kartashov Y V and Skryabin D V 2019 *Phys. Rev. Lett.* **122** 083902
[40] Harder T H *et al* 2021 *ACS Photonics* **8** 1377
[41] Dusel M *et al* 2021 *Nano Lett.* **21** 6398
[42] Su R, Ghosh S, Liew T C H and Xiong Q 2021 *Sci. Adv.* **7** 8049
[43] Solnyshkov D D, Malpuech G, St-Jean P, Ravets S, Bloch J and Amo A 2021 *Opt. Mater. Express* **11** 1119
[44] Kozin V K, Iorsh I V, Kibis O V and Shelykh I A 2018 *Phys. Rev.* B. **97** 035416
[45] Downing C A, Sturges T J, Weick G, Stobińska M and Martín-Moreno L 2019 *Phys. Rev. Lett.* **123** 217401
[46] Su W P, Schrieffer J R and Heeger A J 1979 *Phys. Rev. Lett.* **42** 1698
[47] Su W P, Schrieffer J R and Heeger A J 1980 *Phys. Rev.* B **22** 2099
[48] Zak J 1989 *Phys. Rev. Lett.* **62** 2747
[49] Asbóth J K, Oroszlány L and Pályi A 2016 *A Short Course on Topological Insulators* (Springer)
[50] Solnyshkov D D, Nalitov A V and Malpuech G 2016 *Phys. Rev. Lett.* **116** 046402
[51] Jiao Z *et al* 2021 *Phys. Rev. Lett.* **127** 147401
[52] Pannir-Sivajothi S, Stern N P and Yuen-Zhou J 2023 *Nanophotonics* **12** 3109
[53] Kozin V K, Shelykh I A, Nalitov A V and Iorsh I V 2018 *Phys. Rev.* B **98** 125115
[54] Rojas-Sánchez J A, Jomaso Y A G, Vargas B, Domínguez D L, Ordonez-Romero C L, Lara-García H A, Camacho-Guardian A and Pirruccio G 2023 *Phys. Rev.* B **107** 125407
[55] Pickup L, Sigurdsson H, Ruostekoski J and Lagoudakis P G 2020 *Nat. Commun.* **11** 4431
[56] Pieczarka M *et al* 2021 *Optica* **8** 1084
[57] Jang S J and Mennucci B 2018 *Rev. Mod. Phys.* **90** 035003
[58] Ribeiro R F, Martínez-Martínez L A, Du M, Campos-Gonzalez-Angulo J and Yuen-Zhou J 2018 *Chem. Sci.* **9** 6325
[59] Schröter M, Ivanov S D, Schulze J, Polyutov S P, Yanc Y, Pullerits T and Kühn O 2015 *Phys. Rep.* **567** 1
[60] Tavis M and Cummings F W 1969 *Phys. Rev.* **188** 692
[61] Dicke R H 1954 *Phys. Rev.* **93** 99
[62] Liu J, Zhao Q and Wu N 2020 *J. Chem. Phys.* **153** 074108